Construction and Building Materials 95 (2015) 437–447

Contents lists available at ScienceDirect

Construction and Building Materials

journal homepage: www.elsevier.com/locate/conbuildmat

A unified failure criterion for unstabilized rammed earth materials upon varying relative humidity conditions

Pierre Gerard *, Mohamed Mahdad, Alexandre Robert McCormack, Bertrand François

Université libre de Bruxelles (ULB), BATir Department – Laboratory of GeoMechanics (LGM), Av. F Roosevelt 50 – CPI 194/02, 1050 Brussels, Belgium

HIGHLIGHTS

- Impact of the hygroscopic conditions on the strength of earthen constructions is analyzed.
- Compressive and tensile strengths are determined on earthen materials upon varying relative humidity.
- Suction plays an important role on the strength of the material.
- A unified failure criterion including the effect of the suction inside the stress state is proposed.

ARTICLE INFO

Article history:
Received 9 March 2015
Received in revised form 10 June 2015
Accepted 14 July 2015
Available online 25 July 2015

Keywords:
Unstabilized rammed earth material
Compressive strength
Tensile strength
Suction
Failure criterion
Effective stress

ABSTRACT

Uniaxial compression tests and indirect tensile tests are performed on compacted clayey silt samples upon varying suctions in order to assess the influence of changes in the relative humidity conditions on the strength of unstabilized rammed earthen building materials. The results show that suction plays an important role on the strength of the material. Also the ability of the Belgian clayey silt to develop sufficient mechanical strength to be used as an unstabilized earthen construction material is demonstrated whatever the relative humidity conditions, excepted the fully water saturated state. The experimental data are interpreted in the context of unsaturated soil mechanics using the generalized effective stress concept. This constitutive framework allows defining a unified failure criterion predicting the strength of the earthen building material as a function of the environmental hygroscopic conditions.

1. Introduction

Earthen construction is an ancient technique that is experiencing a renascence today thanks to the energy performance of this material and its potential for recycling. The material is locally available and the energy use for its manufacturing (i.e., embodied energy) is very limited [31,32]. Soil is one of the most predominant materials on earth. It is abundant and can be considered universal to some extents that avoid dependency on importation. Earth materials demonstrate a satisfactory thermal inertia and good hygroscopic properties that allows a natural hygrothermal regulation of buildings [2,7]. Those advantages open large perspective for the use of earthen materials in the field of building engineering.

In order to provide appropriate mechanical properties, the earthen materials, forming the wall, must be installed in a proper way in order to optimize the density and the water content. Among different kinds of earthen constructions (see [21] for an exhaustive review), rammed earth is the technique that consists in forming the wall by compacting moist soil between temporary forms. For "unstabilized" rammed earth, the system does not require any additional binder elements (such as cement or lime). A part of the cohesion is brought by the argillaceous materials in combination with the compaction process that provides the required density. The compaction should be performed at an adequate water content of the soil that allows optimizing the density for a given energy of compaction. In addition to the natural binding effect of the argillaceous material, capillary cohesion contributes, for a big part, to the total strength of the materials [17,28]. This is related to the internal suction which is related to the co-existence of gas and liquid phases in the void space.

However, after the construction, external rammed earth walls can be subject to large changes in humidity and incident wetting from rainfall. Those perpetual changes of environmental conditions induce continuous changes of the water retention conditions of the wall that affect the durability of the constructions. Characterization

* Corresponding author.
E-mail address: piergera@ulb.ac.be (P. Gerard).

http://dx.doi.org/10.1016/j.conbuildmat.2015.07.100
0950-0618/

of the erosion has been performed on earthen walls in climatic chamber [19] or under in-situ conditions [11], but few studies focus directly on the impact of the change in relative humidity on the internal suction, and so on the strength of the wall.

The impact of those earthen constructions – atmosphere interactions on the strength has been investigated experimentally under laboratory conditions by Jaquin et al. [23], who performed unconfined compression tests on earthen materials samples air-dried to different target water contents. The suction (<1 MPa) was measured by means of high capacity tensiometers. This study quantified the increase in the strength and stiffness when the water content decreases. However, in that study, the water content varied between 5.5% and 10.2%, while the water content of an unstabilized rammed-earth construction subject to atmospheric conditions is generally lower (1–2%) [10]. Bui et al. [12] determined the unconfined strength of different soil samples (sand, clay) with a greater range of water content (from a wet state after manufacturing $w = 11\%$ to a dry state in atmospheric conditions $w = 1$–2%). This study confirmed that suction plays an important role on the strength of the material, but highlighted also that a slight increase in moisture content of dry rammed-earth walls (water content not exceeding 4%) due to rainfall or change of relative humidity in the atmosphere is not followed by a sudden drop in the wall strength.

This literature review reveals therefore first the scarcity of experimental procedure replicating the prevailing climatic conditions in different regions of the world, and quantifying the evolution of the unstabilized earthen materials strength with the atmospheric conditions. On the other hand no unified failure criterion has been formulated to characterize the effect of the suction and capillary cohesion on the strength of these materials.

The first objective of the present study is to evaluate, from an experimental point of view, the ability of a representative Belgian clayey silt to develop sufficient mechanical strength under variable relative humidity conditions to be used as an unstabilized rammed earthen building materials. To do so, the optimum water content for dynamic compaction is determined and the evolution of the strength as a function of the atmospheric relative humidity is characterized through uniaxial compression tests and indirect tensile tests.

Then, the second objective is to propose a constitutive framework, based on the concepts of unsaturated soil mechanics, able to predict the failure criterion of unstabilized rammed earthen materials, including the effect of capillary and intrinsic cohesion through the generalized effective stress approach for unsaturated soil. Such a failure criterion will be useful to verify the stability of earthen constructions under the combination of various loadings (and so various applied stresses on the material) and various atmospheric conditions (and so various strength of the materials). So, this approach unifies the hygroscopic and mechanical effects on the rammed earth in a single failure criterion.

The paper is organized as follows. The first section presents the used soil and its geotechnical properties. Then, the different experimental techniques are described and the obtained results are presented. Finally, the results are interpreted in the context of unsaturated soil mechanics in order to provide a coherent constitutive framework that allows predicting the strength of the earthen building material as a function of the environmental hygroscopic conditions.

2. Materials

2.1. Identification parameters

The soil examined in this research is a clayey silt (Unified Soil Classification System (USCS): clay of low plasticity (CL)) from the region of Marche-Les-Dames (Belgium). This soil has already been the subject of many studies in the past for other applications [20,37]. So, it represents a referential material which has been already extensively characterized for other purposes. Its index properties are: liquid limit (w_L) = 32.5%; plasticity index (IP) = 15%. The grain-size distribution curve is reported in Fig. 1. The clayey fraction represents 13%, the silty one about 64% and the sandy one about 26%. Walker et al. [38] and Hall and Djerbib [18] summarized a series of recommendations on the grain-size distribution of soils particularly well adapted for earthen constructions. Even though most of the guidelines for a suitable rammed earth particle size distribution recommend an inert aggregate fraction of gravel, the Marche-Les-Dames silt used in this study does not contain any gravel. Nevertheless the particle size distribution of the Marche-les-Dames silt approaches the one proposed by Alley [1] and will show his relevance for earthen constructions (i.e., dry density, strength) in the next sections. Those good properties are due to the spread grain size distribution of this natural clayey silt that induces a good interlocking of grains after compaction.

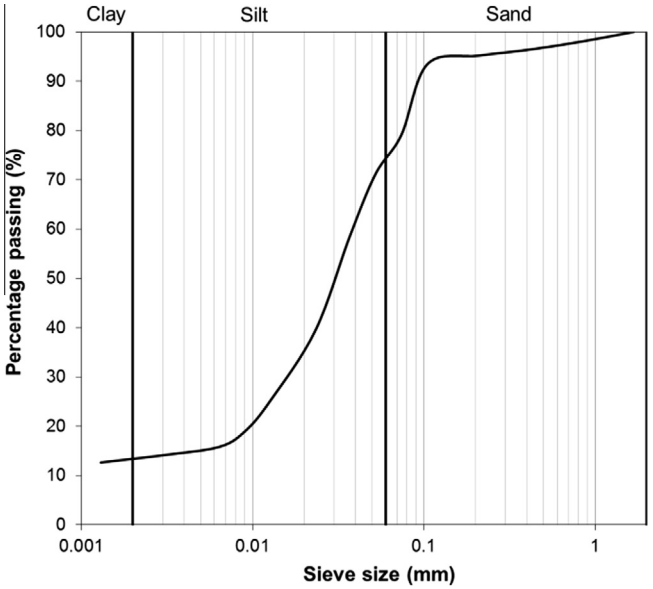

Fig. 1. Particle size distribution of the studied soil.

The normal Proctor compaction curve [4] is reported in Fig. 2. The optimum water content is 15% and the optimum dry density is 18.40 kN/m^3.

2.2. Optimized compaction conditions

Even if the normal Proctor compaction test constitutes a widely used standard for the geotechnical earthworks (e.g., embankment, road, etc.), this method is generally not considered in the context of earthen materials. Indeed, the targeted properties of an earthen wall largely differ from the properties expected for geotechnical works. To reach the target strength, we have to apply far greater compaction energy.

It is why other compaction methods have been already proposed as the heavy manual compaction test or the vibrating hammer test [34]. In this paper, a third compaction process has been used. The soil was dynamically compacted by sequentially ramming the soil in layers with a 2.5 kg Proctor hammer directly inside two kinds of mould: 36 mm in diameter and 72 mm in height for the uniaxial compression test (compacted in 3 layers) and 36 mm in diameter and 22 mm in height for indirect tensile test

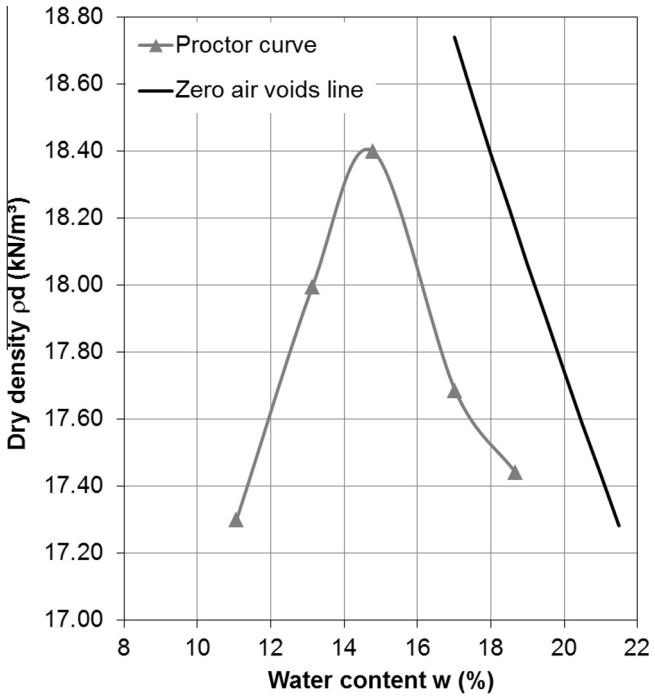

Fig. 2. Normal Proctor compaction curve of the studied soil.

(compacted in 1 layer). The effect of the size sample will be discussed further.

The compaction of each layer was achieved until the handle of the hammer "rings" when dropped onto the compacted soil, which is considered as the indication of full compaction having being attained [18,38]. So doing, we can expect to obtain a material which is as dense as possible. The dynamic compaction in multiple layers was to mimic the same ramming process in-situ. The proctor hammer would however impact the soil via a metal rod closely fitting the mould, so the compaction process would be considered confined as the soil did not have space for displacement.

To determine the optimum initial water content samples were prepared at 8 different water contents (dried soil, 2%, 4%, 6%, 8%, 10%, 12%, 14%). To do so, dry soil was mixed with the required quantity of distilled water; mellowed in a plastic bag during 24 h to obtain a homogeneous distribution of the water in the soil; then compacted. The samples at a theoretical 0% and 2% of water contents were unusable as the samples became laminated and quickly dismantled at the limits of their compacted layers. The samples were then tested upon uniaxial compression loadings in order to evaluate their uniaxial compression strength (UCS) as a function of their water contents at compaction. For each compression, 3–4 samples were tested under unconfined compression for statistical consistency. It is to mention that the spreading of the strength never exceeds 10% of the mean value, which demonstrates a good reproducibility of the results. The obtained mean UCS is reported in Fig. 3a together with the obtained dry density.

For the sake of comparison, the mean UCS obtained on samples compacted at much lower dry density, 1732 kg/m^3, at different water contents are reported in Fig. 3b. This dry density is close to the optimum Proctor dry density of the soil (Fig. 2).

First of all, the results show the relevance of the compaction method adapted for earthen construction. The process for earthen construction (Fig. 3a) provides much denser samples than the normal Proctor method (Fig. 2) with the consequence that the water content of rammed earth is much lower that the optimum Proctor water content. It is why the standard geotechnical normal Proctor test is considered as unsuitable for the study of rammed earth.

On the other hand the comparison between Fig. 3a and b clearly demonstrates the drastic effect of soil density on its strength. This 'as-compacted UCS' reaches barely 1.4 MPa upon a dry density of 1732 kg/m^3 at 6% of water content. On the contrary, when the soil is compacted until bouncing of the hammer, the samples develop an 'as-compacted UCS' that may reach 3.8 MPa for a dry density of 2020 kg/m^3 when compacted at 8% of water content (Fig 3a).

The curve of UCS as a function of the water content at compaction exhibits a large zone upon which the reached UCS is satisfactory. Indeed, water contents from 4% to 10% provide UCS above 2.5 MPa, which are largely sufficient to be used as an earthen building material. In the next sections, the optimized conditions of compaction (w_0 = 8% and ρ_d = 2000 kg/m^3) have been selected to determine the effect of the hygroscopic variations on the strength. A target dry density slightly lower than the maximum density reached in Fig. 3a was applied in order to take into account some possible losses of efficiency of the compaction process in real in-situ conditions.

3. Methods

3.1. Filter paper

First of all, after compaction, it is important to determine the initial suction of the samples. It constitutes the starting point from which the other hygroscopic conditions will be applied. The measurement of the initial suction of the soil has been carried out by

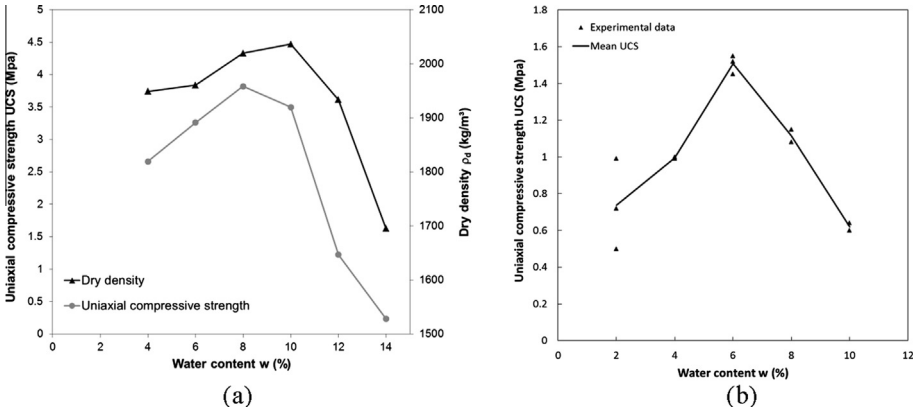

Fig. 3. (a) Uniaxial compressive strength according to the initial water content and the dry density obtained on samples compacted with the process for earthen construction; (b) Mean uniaxial compressive strength according to the initial water content obtained on samples compacted at a density of 1732 kg/m^3.

the filter paper method [14]. Basically, the principle is that the filter paper is put in contact with the soil and when equilibrium is reached, the filter paper and the soil have the same suction. The used filter papers (WHATMAN N° 42) are calibrated in order to be able to deduce the suction based on the water content of the filter paper. Three filter papers are entrapped between two soil samples. The measured filter paper is in the middle while the two other filter papers are used to protect the calibrated filter paper from being contaminated by the soil. The system (filter papers + soil samples) is then sealed into plastic and aluminum films and then surrounded by wax. After seven days, the measured filter paper is weighted to determine its water content. Based on the water content of the filter paper, the suction is found from the calibration curve.

3.2. Control of suction

The control of suction by the relative humidity technique (also called vapor transfer technique) is based on the regulation of the relative humidity of the atmosphere surrounding the sample by means of an aqueous solution of a given chemical compound (a product at various concentrations or different saturated saline solutions) [16]. According to the relative humidity of the air, water exchanges occurring by vapor transfers between the sample and its surrounding induce a given suction at equilibrium within the sample.

The relationship between suction at equilibrium inside the soil sample and the relative humidity of the surrounding air is given by Kelvin's law:

$$s = \frac{\rho_w RT}{M_w} \ln \mathrm{RH} \tag{1}$$

where s is the suction, R is the constant of perfect gases (R = 8.3143 J/mol/K), T is the temperature in Kelvin, M_w is the molar mass of water (M_w = 0.018 kg/mol), ρ_w is the bulk density of water (ρ_w = 1000 kg/m^3), and RH is the relative humidity.

To influence the relative humidity of air surrounding the sample, saturated saline solutions were used: K_2SO_4 (RH = 97%), KNO_3 (RH = 92%), KCl (RH = 85%), NaCl (RH = 75%). Also, RH = 40% was reached by placing the samples under ambient conditions in a room of the laboratory in which temperature and humidity remain constant. For a temperature of 20 °C, it is possible to deduce the imposed suction through Eq. (1), as reported in Table 1.

Also, a last hydraulic condition was obtained by sample saturation. The samples are surrounded by a rubber membrane and installed in a confining cell. The lower and upper surfaces of the cylindrical sample (which are not encased with the rubber membrane) are in contact with porous stones that are connected to the drainage system. The porous stones permit to get a homogeneously-distributed water pressure at the top and the bottom of the sample. A confining pressure of 200 kPa was applied in the confining cell while a water pressure of 190 kPa was applied on the lower porous stone. It corresponds to an effective stress of 10 kPa. Considering the density of the material, this low effective confining pressure during saturation does certainly not affect the microstructure of the specimen. The upper porous stone is in contact with atmospheric pressure in order to allow air bubble (initially entrapped in the soil pores) to be expelled out of the sample. The saturation is reached when the flowrate of water injected in the sample through lower porous stone is equal to the flowrate of water measured through the upper porous stone. After dismantling the system, the degree of saturation is also checked by measuring and weighting the sample.

Table 1
Suction imposed by means of the different saturated saline solutions.

Saturated saline solutions	Relative humidity RH (%)	Suction (MPa)
K_2SO_4	97	4.17
KNO_3	92	11.43
KCl	85	22.29
NaCl	75	39.46
(Ambient air)	40	125

3.3. Uniaxial compression test

The scope of the uniaxial compression test is to determine the uniaxial compressive strength (UCS) of soil samples with unrestricted horizontal deformation. The displacement of the piston was at 0.0667 mm/min and the stress and strain were monitored every second. The associated parameters, axial strain ε_a and stress σ_{UCS}, are calculated as:

$$\varepsilon_a = \frac{\Delta H}{H_0} \tag{2}$$

where ΔH is the vertical displacement of the piston (corresponding to the shortening of the sample) and H_0 is the initial height of the sample.

$$\sigma_{UCS} = \frac{F}{A_c} \tag{3}$$

where $A_c = A_0(1 - \varepsilon_a)$ under the assumption of constant volume of the sample during loading. A_0 is the initial area of the sample while A_c is the equivalent section, different from initial section due to Poisson effect during compression. F is the force applied by the piston.

It is worth to note that the size of the samples (D = 36 mm; H = 72 mm) is consistent with the recommendations of Aubert et al. [6] on the geometry of the samples. A slender ratio (H/D) of 2 is indeed necessary for the determination of the uniaxial compressive strength of earthen materials. On the other hand Ciancio and Gibbings [15] have studied the influence of the sample size on its strength. They tested several samples manufactured with different diameters and a constant slender ratio of 2. While an inverse relationship between strength and specimen size is generally observed on concrete samples [13], they showed that the strength of earthen materials is not influenced by the size.

3.4. Indirect tensile test

In order to determine the uniaxial tensile strength of earthen materials, indirect tensile tests (also called Brazilian tests) have been conducted. The test is valid for the materials exhibiting relative brittle failure which is the case for highly compacted earthen materials [30]. It produces tensile failure in the end faces of cylindrical samples subject to compressive force F along their lengths L. Under such loadings, the minor principal stress is the horizontal stress, in tension, which corresponds to the tensile strength σ_t:

$$\sigma_3 = \sigma_h = -\frac{2F}{\pi dL} = \sigma_t \tag{4}$$

and the major principal stress is the vertical one, in compression:

$$\sigma_1 = \sigma_v = \frac{6F}{\pi DL} \tag{5}$$

with D the diameter of the sample.

According to the soil mechanics stress convention, compressive stress is assumed positive while tensile stress is negative.

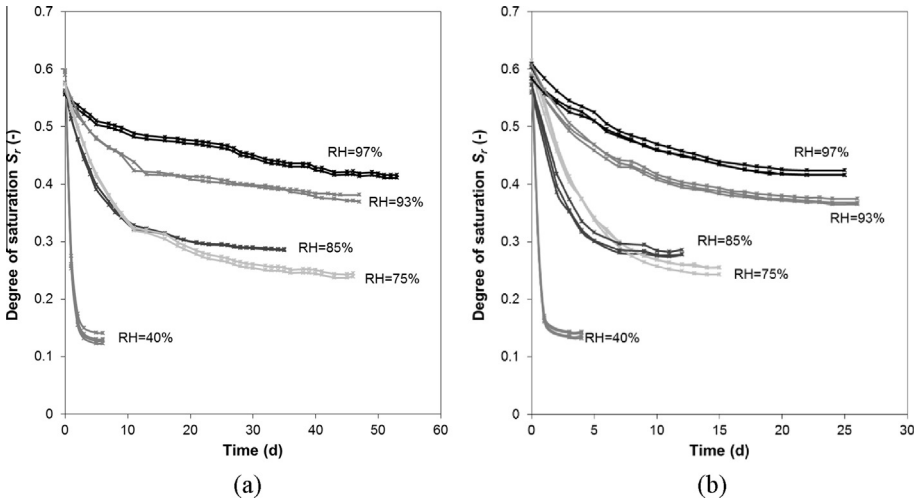

Fig. 4. Kinetics of desaturation of (a) large samples (D = 36 mm; H = 72 mm) and (b) small samples (D = 36 mm; H = 22 mm).

4. Experimental results

4.1. Water retention curve

Before testing the mechanical strength of the soil, it is important to characterize the water retention behavior because in the framework of unsaturated soil mechanics, water retention and mechanical behaviors are interconnected [33]. The amount of water stored in the specimen affects the capillary cohesion and has, in turn, a direct influence on the strength.

First, just after compaction, the initial water content is the imposed water content at compaction (w_0 = 8%) while the suction has been evaluated at 2.4 MPa by the filter paper method. This suction corresponds to the 'as-compacted' state of the material before any effect of the relative humidity of the atmosphere.

As described in Section 3.2, the soil suction was imposed through the control of relative humidity. Soil samples prepared at the two different dimensions and compacted according to the methodology described in Section 2.2 were placed in desiccators with saturated salt solutions (or at ambient laboratory conditions for RH = 40%) and were weighted every day until reaching a constant weight. Owing to the saturated saline solutions chosen (Table 1) and the initial suction of the samples (2.4 MPa), all the samples were subjected to drying into the desiccators or at ambient conditions. For each relative humidity and for each sample size, two to four samples were dried for statistical consistency. The kinetics of drying is reported in Fig. 4. The curves are expressed in terms of degree of saturation S_r (i.e., the ratio between the volume of water and the volume of voids) in order to provide a relative quantity, unaffected by the size of the sample. It is worth to mention that this degree of saturation is "uncorrected" in the sense that it assumes a constant volume of the sample upon drying, because the exact volumes of the samples were only measured once the equilibrium was reached. The obtained curves show very good reproducibility. Obviously, the smallest samples dry faster.

After equilibrium, 3 diameters (top, middle and bottom of the sample) and the height were measured for each sample with a caliper. The volumetric strain upon drying is reported in Fig. 5. Upon drying, the specimen exhibit relatively low volume variations (less than 1%) while upon saturation, the volume changes are much larger (more than 3%). This is because the soils have been highly compacted which makes the possibility of shrinkage very limited.

Fig. 6a and b report the water retention curve expressed in terms of water content and degree of saturation, respectively. Under ambient conditions (s = 125 MPa), the soil reaches very dry states (S_r = 12%).

4.2. Uniaxial compressive strength

Fig. 7a–g report the stress–strain curves obtained during uniaxial compression tests on soil specimen at different initial suctions. The results exhibit the following trends:

- The UCS increases with suction: dryer is the soil and higher is the strength.
- However, in the same time, the brittleness also increases with suction: the material is less and less ductile when the amount of water in the soil decreases.
- Upon saturated conditions, the strength is almost zero while it is very ductile. It demonstrates the strong contribution of capillary cohesion on the strength of the material.

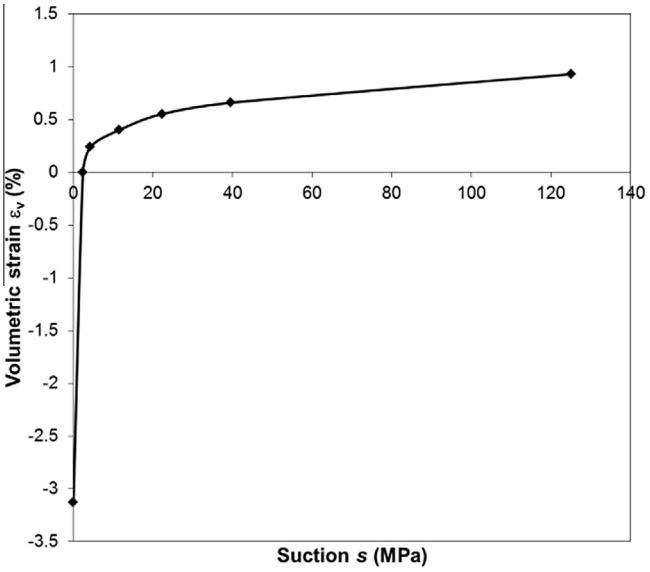

Fig. 5. Volumetric strain measured after relative humidity equilibrium according to the suction.

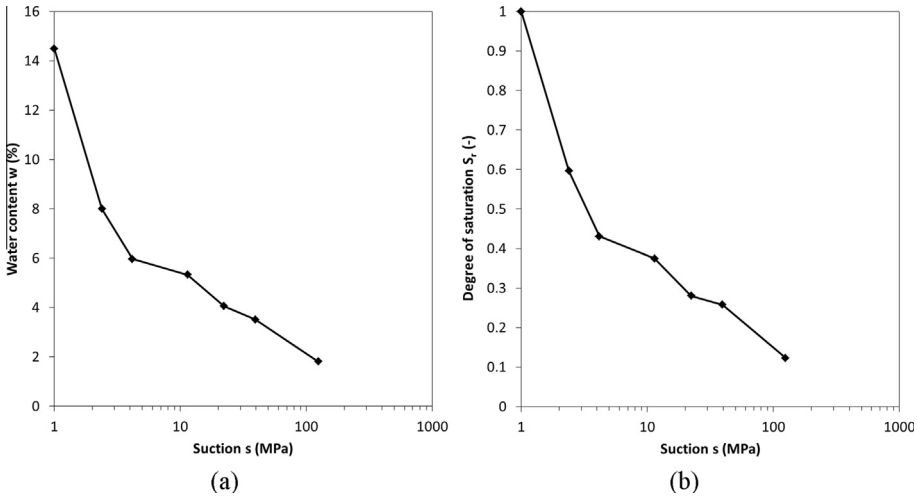

Fig. 6. Retention curve expressed in terms of (a) water content and (b) degree of saturation according to the suction.

Fig. 8 summarizes the obtained UCS as a function of the applied suction. Suction is reported on a logarithmic scale. Saturated conditions (for which suction is almost zero) were arbitrary linked to suction of 1 MPa, for the convenience of the representation. Excepted for the results at 4.17 MPa of suction, a logarithmic regression curve provides a good estimation of the obtained UCS. The points out of the trend at 4.17 MPa (RH = 97%) can probably be explained because of the precision of the relative humidity technique at low suctions. This is a well-known drawback of this technique which is not adequate to apply low suctions. A small error in the imposed relative humidity induces a large approximation in the imposed suction (e.g., 1% of relative uncertainty on RH leads to 1.38 MPa of absolute uncertainty for the suction) [16].

4.3. Tensile strength

Contrary to uniaxial compression test, indirect tensile test does not allow to obtain a representative strain state based on the displacement of the piston. Consequently, stress–strain relationships are not presented but only the ultimate tensile strength is reported in Fig. 9. Again, logarithmic regression curve provides a good estimation of the evolution of the strength as a function of suction, except for the points at 4.17 MPa (RH = 97%), for the same reasons than exposed before.

5. Constitutive framework

5.1. Stress state

Unlike the case of saturated conditions, the soil suction, which is specific to an unsaturated medium, has a direct impact on the state of stress acting at the particle–particle contact. Consequently, the macroscopic mechanical behavior of the soil is directly affected by the suction level. The framework of unsaturated soil mechanics provides two main families of approaches to analyze the mechanical response of soils: the two independent stress variables and the generalized effective stress [22]. The choice of stress framework appears to be mostly a matter a convenience. On the one hand, approaches with two independent stresses use measurable stresses which have an experimental significance [17]. On the other hand, a generalized effective stress converts a multi-phase porous media into a mechanically equivalent, single-phase, single-stress state continuum which has noticeable advantages in the elaboration of a constitutive framework [26,27,33].

For the purpose of constitutive analysis, an approach using a generalized effective stress is used. In the sense of Terzaghi's [35] definition, the effective stress should be such that "all the measurable effects of a change in stress, such as compaction, distortion and a change in shearing resistance are exclusively due to a change in the effective stress". Consequently, the effective stress governs the elastic, elasto-plastic and strength behaviors of the soil. In our study, we are dealing with strength. The objective of this section is to find an expression of generalized effective stress that permits to obtain a unique failure criterion that is unaffected by suction and degree of saturation, when it is expressed in this new stress reference. In other words, the dependency of the water retention conditions on the strength is directly included in the stress definition and is not explicitly taken into account in the expression of the failure criterion.

To do so, it is proposed to start from the general expression of generalized effective stress σ'_{ij} as originally proposed by Bishop [8]:

$$\sigma'_{ij} = \sigma_{ij} + \chi s \delta_{ij} \tag{6}$$

where χ, called the effective stress parameter, varies with the degree of saturation [8,29], from zero for dry soil to unity for fully saturated conditions. σ_{ij} is the total stress tensor (i.e., the stress applied externally) and δ_{ij} is the Kroenecker symbol (=0 when $i \neq j$ and =1 when $i = j$). This Bishop's effective stress implies that the mechanical response is directly linked to the water retention behavior through the parameter χ. It translates the fact that the relative amounts of the pore air and pore water phases play a key role in the mechanical properties of the unsaturated soil.

One of the consequences of this generalized effective stress for unsaturated soil is that, even when a sample is free of stress at its boundary, the internal stress is not zero but depends on the water retention conditions through the product between the suction and the effective stress parameter χ. In other words, suction provides a kind of internal confining stress to the specimen. Samples which are unconfined externally may be considered as stress-confined when it is expressed in this generalized effective stress reference. Consequently, generalized effective stress state experienced by specimen during both uniaxial compression tests and indirect tensile tests can be reported in the Mohr plane with Mohr circles which are shifted to the right by an amount equal to χs, as schematically represented in Fig. 10.

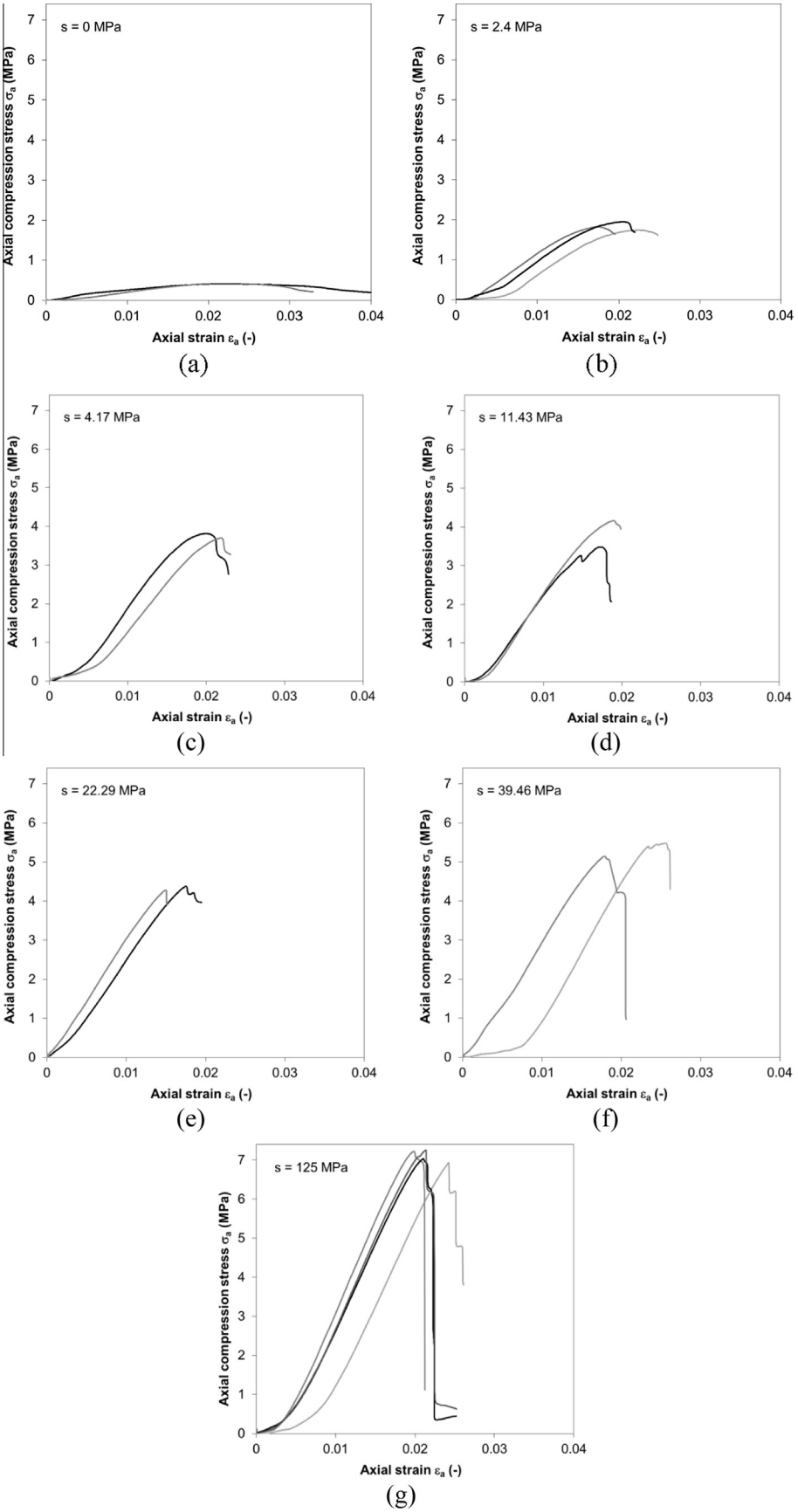

Fig. 7. Stress–strain curves during uniaxial compression test at different initial suctions (a) $s = 0$ MPa – saturated conditions; (b) $s = 2.4$ MPa – 'as compacted" state; (c) $s = 4.17$ MPa; (d) $s = 11.43$ MPa; (e) $s = 22.29$ MPa; (f) $s = 39.46$ MPa; (g) $s = 125$ MPa – ambient conditions.

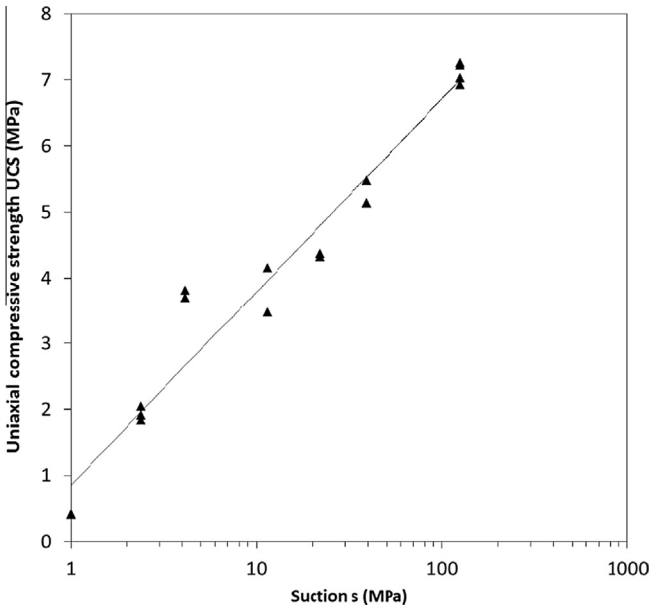

Fig. 8. Uniaxial compressive strength according to the imposed suction.

The question is now to find a suitable expression of χ as a function of the degree of saturation S_r that permits a shift of the obtained Mohr circles at failure that fulfills a unique failure criterion.

5.2. Unified failure criterion

The first step towards the definition of a unified failure criterion for the studied rammed earth material consists in the determination of the intrinsic strength parameters, friction angle φ and cohesion c. To do so, 4 consolidated and undrained (CU) triaxial tests have been performed on saturated samples at different confining pressures σ_3 (50, 100, 200 and 300 kPa), with measurement of the pore pressures evolution during shearing. The stress paths followed by the different specimen during shearing and expressed in terms of effective stress are represented on Fig. 11 in the $(p' - q)$

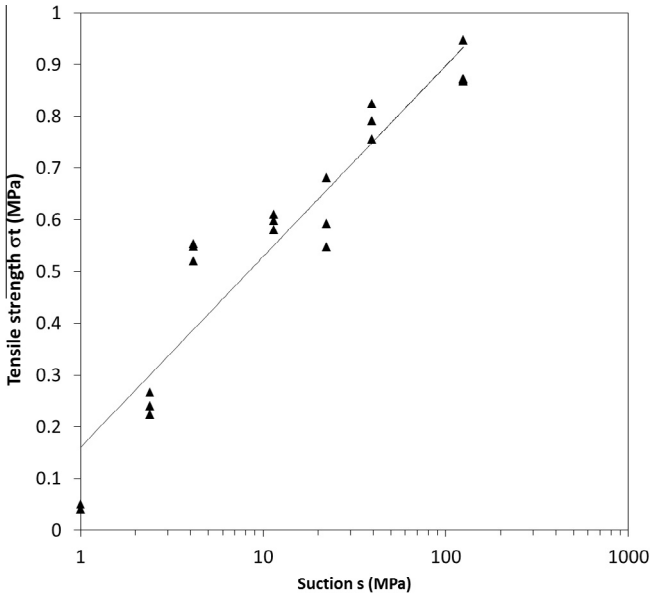

Fig. 9. Tensile strength according to the imposed suction.

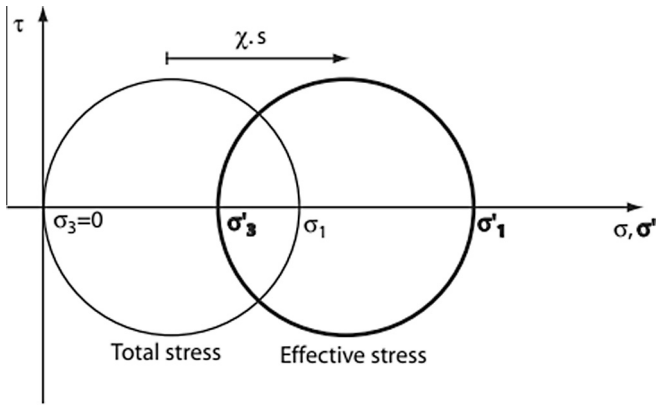

Fig. 10. Mohr circles experienced during uniaxial compression test expressed in terms of total stress and generalized effective stress.

space with p' the mean effective stress and q the deviatoric stress. In triaxial conditions, p' and q are expressed as:

$$p' = \frac{\sigma'_1 + 2\sigma'_3}{3} \tag{7}$$

$$q = \sigma'_1 - \sigma'_3 \tag{8}$$

with those stress variables, the failure criterion reads:

$$q = k + Mp' \tag{9}$$

with $M = \frac{6\sin\varphi}{3-\sin\varphi}$ and $k = M\frac{c}{\tan\varphi}$

Considering the maximum ratio σ'_3/σ'_1 as the ultimate stress state [5], this leads to $M = 1.483$ and $k = 12.365$ (Fig. 11) that corresponds to $\varphi = 36.5°$ and $c = 6.2$ kPa.

Secondly, when the intrinsic criterion is defined, the purpose being to obtain a unique failure criterion, the objective is to find the value of χ, expressed as a function of S_r, that allows to translate horizontally the corresponding Mohr circle at the ultimate stress state expressed in total stress on the failure criterion. The horizontal distance between the Mohr circle expressed in total stress and

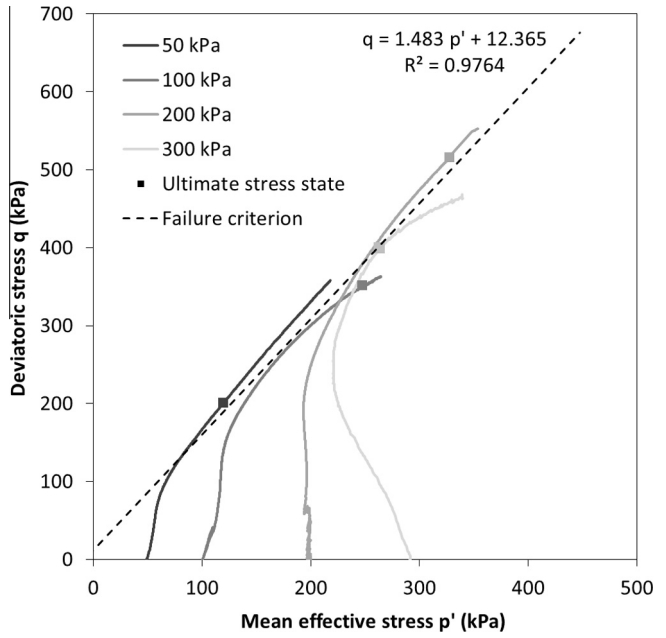

Fig. 11. Failure criterion obtained from stress paths of 4 consolidated undrained (CU) triaxial tests upon saturated conditions.

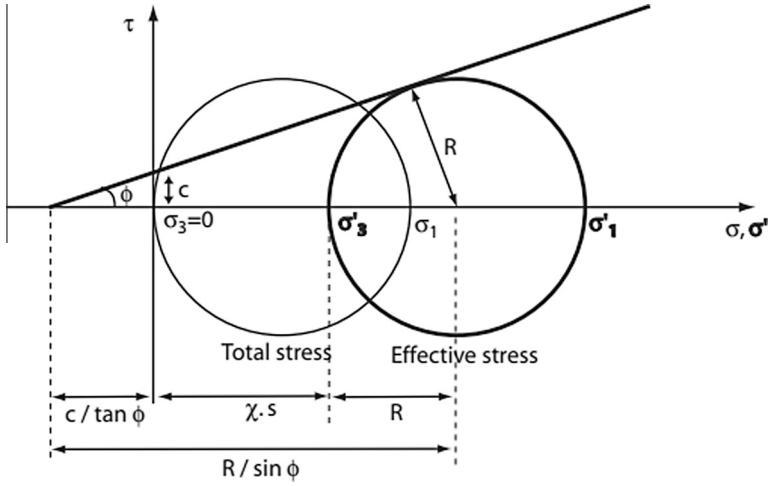

Fig. 12. Mohr circle at failure for uniaxial compression test expressed in total stress and effective stress.

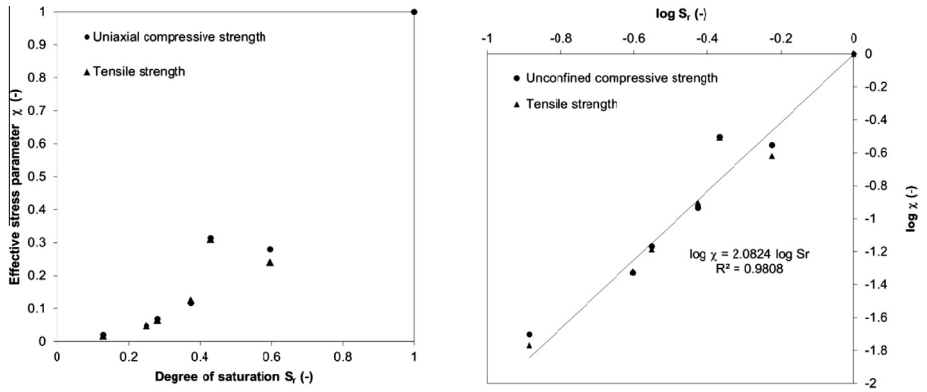

(a) (b)

Fig. 13. Degree of saturation according to the effective stress parameter χ from both uniaxial compressive strength and tensile strength in normal (a) and logarithmic (b) planes.

the failure criterion is the value χs. Knowing that σ'_3 is expressed as $\sigma'_3 = \chi s$ for the uniaxial compression test and $\sigma'_3 = \sigma_h + \chi s$ for the indirect tensile tests, the value χs can be obtained geometrically from (Fig. 12):

$$\sigma'_3 = \frac{R - c\cos\varphi}{\sin\varphi} - R \tag{10}$$

with $R = \frac{\sigma_1 - \sigma_3}{2}$.

This method can be applied to every single test result to obtain one value of χ per test. Because for each test, the value of the degree of saturation of the sample is measured, it is possible to obtain a set of points in the $\chi - S_r$ plane, as reported in Fig. 13a. It is then decided to find a relation in the form:

$$\chi = (S_r)^{\alpha} \Rightarrow \log\chi = \alpha \log S_r \tag{11}$$

where α is a material parameter which is the slope of the regression line in the plane $\log\chi - \log S_r$ reported in Fig. 13b. This expression fulfills the requirement initially formulated by Bishop [8]: "The effective stress parameter χ varies with the degree of saturation S_r, from zero for dry soil to unity for fully saturated conditions".

In such a way, we find $\alpha = 2.08$. The obtained relationship between χ and S_r is compared, in Fig. 14, with values plotted by Zerhouni [39] in which this relationship is reported for several soils. It is worth to note that, in Fig. 14, the parameter χ was

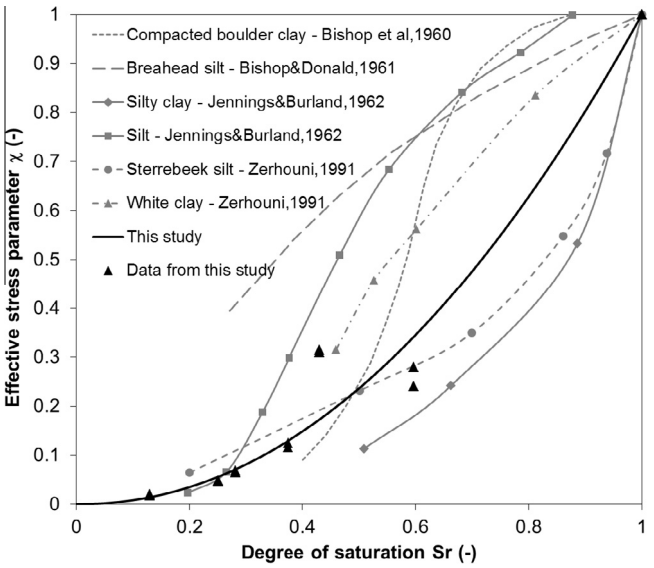

Fig. 14. Effective stress parameter according to the degree of saturation for different soils.

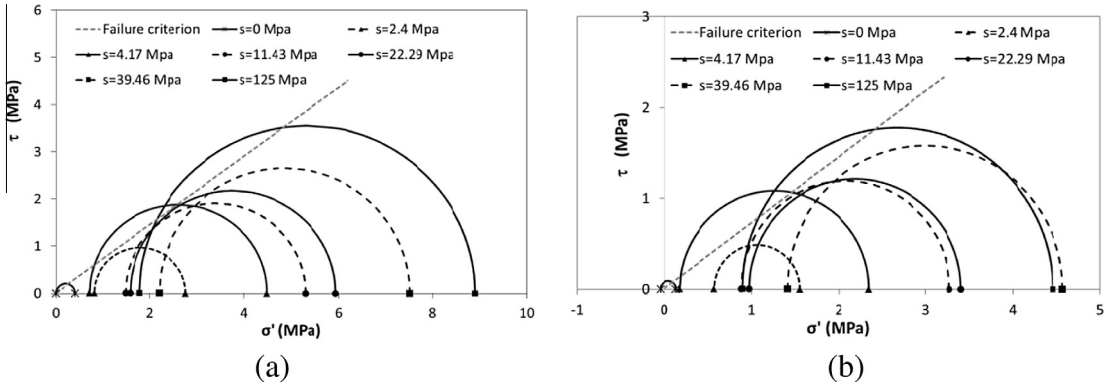

Fig. 15. Mohr circles at failure expressed in terms of generalized effective stress for (a) uniaxial compression tests and (b) indirect tensile tests at different initial suctions.

obtained based on different criteria: the volume change and shear strength [9], comparison between soil response upon change in applied external stress and applied suction [24] or critical state [36]. Our relationship is relatively similar to the ones obtained by Zerhouni [39] on the Sterrebeek silt and by Jennings and Burland [25] on a silty clay. This is totally consistent because those materials have rheological properties very similar to the ones of the soil tested in this study.

Moreover, the obtained trend follows the conceptual model of Alonso et al. [3] with a limited increase of the effective stress parameter for low degree of saturation while the increase is more significant for higher degree of saturation (>0.3–0.4 in our case). The compaction process at relatively low water content induces a double structure to the material with two characteristic sizes of pores (large pores between aggregates and small pores inside aggregates). Consequently, upon low degree of saturation, the water is essentially stored inside the aggregates and this "intra-aggregate" water does not contribute to the macroscopic stress. Upon higher degree of saturation, water floods the "inter-aggregate" voids which contributes more to the increase of the internal stress.

According to the Bishop effective stress framework (Eq. (6)), the gain of effective confinement due to the partially water saturated state corresponds to the product between χ and s. Both of them being related to the degree of saturation (Figs. 6b and 14, respectively), the gain of the mean effective stress can be deduced as a function of the saturation degree of the rammed earth. Upon desaturation, it is usually the suction that increases faster than the decrease of the effective stress parameter which explains why the desaturation produces a gain in strength.

Finally, the set of Mohr circles at failure obtained from uniaxial compression tests and indirect tensile tests are reported in Fig. 15a and b, respectively, using the generalized effective stress reference defined previously:

$$\sigma'_{ij} = \sigma_{ij} + \chi s \delta_{ij} = \sigma_{ij} + S_r^{2.08} s \delta_{ij} \quad (12)$$

As expected, because it was the purpose of this constitutive framework, the obtained Mohr circles at failure fulfill a unique failure criterion based on the cohesion and the friction angle deduced from triaxial tests under saturated conditions (Fig. 11). It is worth mentioning that both uniaxial compression and indirect tensile tests upon saturated conditions do not fit well the failure criterion. It is explained by the probable undrained conditions of the saturated samples under such loadings that makes the interpretation in effective stress inappropriate.

6. Conclusions

The tensile and compressive strengths of unstabilized rammed earthen building materials are strongly affected, not only by the density of the material, but also by the relative humidity conditions. In this study, the hygroscopic behavior is taken into account through the water retention curve that relates the degree of saturation to the suction. This curve has a significant impact on the internal stress state of the material which, in turn, affects its mechanical behavior.

We demonstrated that a framework based on the concepts of unsaturated soil mechanics using a generalized effective stress is particularly well-suited to provide a unified failure criterion including the effect of the suction inside the stress state.

So doing, suction multiplied by the effective stress parameter χ (that is a function of the degree of saturation) plays the same role than a confining pressure. Consequently, suction provides additional strength to the material by mobilizing internal friction between grains. Moreover, we demonstrate the uniqueness of the obtained failure criterion in the sense that it gathers the strengths obtained from uniaxial compression tests and indirect tensile test into a single criterion.

A practical outcome of this unified failure criterion is the estimation of the rammed earth constructions stability under varying atmospheric conditions. Calculations of suction distribution within an earthen construction under varying outer and inner relative humidities and temperatures can be now directly related to strength distribution and evolution. Combining this information with the stresses distributions within the same construction under various loadings allows designing suitable and sustainable earthen structures able to resist to changes in their moisture contents and so to modifications of their strengths.

Acknowledgements

The authors wish to acknowledge Mir Amid Hashemi Afrapoli for the technical support in the completion of some experimental tests.

References

[1] P.J. Alley, Rammed Earth construction, New Zealand Eng. 3 (6) (1948) 582.
[2] D. Allinson, M. Hall, Hygrothermal analysis of a stabilised rammed earth test building in the UK, Energy Build. 42 (2010) 845–852.
[3] E.E. Alonso, N.M. Pinyol, A. Gens, Compacted soil behaviour: initial state, structure and constitutive modelling, Géotechnique 63 (6) (2013) 463–478.
[4] ASTM D 1557–02. Standard test methods for laboratory compaction characteristics of coil using modified effort.
[5] ASTM D 4767-95. Standard test method for consolidated undrained triaxial compression test for cohesive soils.
[6] J.E. Aubert, A. Fabbri, J.C. Morel, P. Maillard, An earth block with a compressive strength higher than 45 MPa!, Constr Build. Mater. 47 (2013) 366–369.
[7] C. Beckett, D. Ciancio, A review of the contribution of thermal mass to thermal comfort in rammed earth structures, in: 2nd International Conference on Sustainable Built Environment, Sri Lanka, 2012, pp. 12.
[8] A.W. Bishop, The principle of effective stress, Tecnisk Ukeblad 39 (1959) 859–863.

[9] A.W. Bishop, I. Alpan, G.E. Blight, I.B. Donald, Factors controlling the strength of partly saturated cohesive soils, in: Conference Shear Strength Cohesive Soils, ASCE, 1960, pp. 503–532.
[10] Q.B. Bui, J.C. Morel, S. Hans, N. Meunier, Compression behaviour of nonindustrial materials in civil engineering by three scale experiments: the case of rammed earth, Mater. Struct. 42 (8) (2009) 1101–1116.
[11] Q.B. Bui, J.C. Morel, B.V. Venkatarama Reddy, W. Ghayad, Durability of rammed earth walls exposed for 20 years to natural weathering, Build. Environ. 44 (2009) 912–919.
[12] Q.B. Bui, J.C. Morel, S. Hans, P. Walker, Effect of moisture content on the mechanical characteristics of rammed earth, Constr. Build. Mater. 54 (2014) 163–169.
[13] J.H. Bungey, S.G. Millard, Testing of Concrete in Structures, Taylor & Francis, 1996.
[14] R.J. Chandler, C.I. Gutierrez, The filter paper method of suction measurement, Géotechnique 36 (1986) 265–268.
[15] D. Ciancio, J. Gibbings, Experimental investigation on the compressive strength of cored and molded cement-stabilized rammed earth samples, Constr. Build. Mater. 28 (2012) 294–304.
[16] P. Delage, M.D. Howat, Y.J. Cui, The relationship between suction and swelling properties in a heavily compacted unsaturated clay, Eng. Geol. 50 (1998) 31–48.
[17] D.G. Fredlund, H. Rahardjo, Soil Mechanics for Unsaturated Soils, Wiley, New-York, 1993.
[18] M.R. Hall, Y. Djerbib, Rammed earth sample production: context, recommendations and consistency, Constr. Build. Mater. 18 (2004) 281–286.
[19] M.R. Hall, Assessing the environmental performance of stabilised rammed earth walls using a climatic simulation chamber, Build. Environ. 42 (2007) 139–145.
[20] M.A. Hashemi, T.J. Massart, J.C. Verbrugge, B. François, Influence of the clay content of a lime-treated soil on its compression strength, in: Proceeding of the International Symposium – Ground Improvement Works, vol II, 2012, pp. 365–372.
[21] H. Houben, H. Guillaud, Earth Construction – A Comprehensive Guide, second ed., Intermediate Technology Publications, London, UK, 1996.
[22] R.J. Jardine, A. Gens, D.W. Hight, M.R. Coop, Developments in understanding soil behaviour, in: Advances in Geotechnical Engineering. The Skempton Conference, Thomas Telford, 2004, pp. 103–206.
[23] P.A. Jaquin, C.E. Augarde, D. Gallipoli, D.G. Toll, The strength of unstabilised rammed earth materials, Géotechnique 59 (5) (2009) 487–490.
[24] J.E. Jennings, A revised effective stress law for use in the prediction of the behaviour of unsaturated soils, in: Pore Pressure and Suction in Soils, Butterworths, London, 1960, pp. 26–30.
[25] J.E.B. Jennings, J.B. Burland, Limitations to the use of effective stresses in partly saturated soils, Géotechnique 12 (1962) 125–144.
[26] C. Jommi, Remarks on the constitutive modelling of unsaturated soils, in: Experimental Evidence and Theoretical Approaches in Unsaturated Soils, Trento, 2000, pp. 139–153.
[27] N. Khalili, F. Geiser, G.E. Blight, Effective stress in unsaturated soils: review with new evidence, Int. J. Geomech. 4 (2) (2004) 115–126.
[28] L. Laloui, M. Nuth, B. François, Mechanics of unsaturated soils, in: L. Laloui (Ed.), Mechanics of Unsaturated Materials, Wiley & Sons Inc, 2010, pp. 29–54.
[29] L. Laloui, M. Nuth, On the use of the generalised effective stress in the constitutive modelling of unsaturated soils, Comput. Geotech. 36 (1–2) (2009) 20–23.
[30] D. Li, L.N.Y. Wong, The Brazilian disc test for rock mechanics applications: review and new insights, Rock Mech. Rock Eng. 46 (2) (2013) 269–287.
[31] B. Little, T. Morton, Building with Earth in Scotland: Innovative Design and Sustainability, Scottish Executive Central Research Unit Publication, 2001.
[32] J.C. Morel, A. Mesbah, M. Oggero, P. Walker, Building houses with local materials: means to drastically reduce the environmental impact of construction, Build. Environ. 36 (2001) 1119–1126.
[33] M. Nuth, L. Laloui, Effective stress concept in unsaturated soils: clarification and validation of a unified framework, Int. J. Numer. Anal. Methods Geomech. 32 (7) (2008) 771–801.
[34] J.C. Smith, C.E. Augarde, Optimum water content tests for earthen construction materials, Construct. Mater. 167 (2) (2014) 114–123.
[35] K. Terzaghi, Theoretical Soil Mechanics, Chapman and Hall, London, 1943.
[36] S.K. Vanapalli, D.G. Fredlund, Comparison of empirical procedures to predict the shear strength of unsaturated soils using the soil-water characteristic curve, in: Advances in Unsaturated Geotechnics, GSP 99, ASCE, Reston, 2000, pp. 195–209.
[37] J.C. Verbrugge, R. De Bel, A. Gomes Correia, P.H. Duvigneaud, G. Herrier (2011) Strength and micro observations on a lime treated silty soil, in: Road Materials and New Innovations in Pavement Engineering, pp. 89–96.
[38] P. Walker, R. Keable, J. Martin, V. Maniatidis, Rammed Earth: Design and Construction Guidelines, BRE Bookshop, Watford, UK, 2005.
[39] M.I. Zerhouni, Rôle de la pression interstitielle négative dans le comportement des sols – application au calcul des routes (Ph.D. thesis), Ecole Centrale Paris, 1991.